

## Beam Vacuum System of Brookhaven's Muon Storage Ring\*

H.C. Hseuh, L. Snydstrup and M. Mapes  
AGS Department, Brookhaven National laboratory  
Upton, New York, 1197

RECEIVED  
OCT 30 1995  
OSTI

### Abstract

A storage ring with a circumference of 45 m is being built at Brookhaven to measure the g-2 value of the muons to an accuracy of 0.35 ppm.. The beam vacuum system of the storage ring will operate at  $10^{-7}$  Torr and has to be completely non-magnetic. It consists of twelve sector chambers. The chambers are constructed of aluminum and are approximately 3.5 m in length with a rectangular cross-section of 16.5 cm high by 45 cm at the widest point. The design features, fabrication techniques and cleaning methods for these chambers are described. The beam vacuum system will be pumped by forty eight non-magnetic distributed ion pumps with a total pumping speed of over 2000 l/sec. Monte Carlo simulations of the pressure distribution in the muon storage region are presented.

### I. INTRODUCTION

The principle equipment of the g-2 experiment<sup>1</sup> is the muon ( $\mu^+$  or  $\mu^-$ ) storage ring and its continuous superconducting magnet which bends and stores the injected muon particles. The magnet has a diameter of 14 m and a gap of 18 cm facing the inside of the storage ring. The cross sectional view of the magnet, its cryostats and the muon storage chamber is shown in Fig. 1. A magnetic field of 14.5 KG with a field homogeneity of 1 ppm is required in the muon storage

\*Work performed under the auspices of the U.S. Department of Energy.

region. This field uniformity requirement, which is far more stringent than the  $10^2$  ppm needed for conventional storage rings, rules out the use of any material with magnetic susceptibility higher than 0.001 in the vacuum system.<sup>2</sup> The traditional material used for the construction of the accelerator high vacuum system, such as stainless steel and inconel, can not be employed here. New designs and fabrication procedures using aluminum, titanium, brass, ceramic, and polymeric materials were developed for the vacuum chambers, pumps and other components and are the subjects of this paper.

## II. DESIGN AND FABRICATION OF THE SECTOR CHAMBER

A plan view of the ring vacuum system without the superconducting magnet is shown in Fig. 2. It consists of twelve 28-degree sector chambers, of which ten are identical (i.e., standard). The detail of a standard sector chamber is shown in Fig. 3. The chamber has an arc length of 3.5 m and a rectangular cross-section with an inner vertical height of 13.8 cm. The horizontal width of the chamber varies from 18 cm at the narrowest point to 45 cm at the widest point. This design provides two stepped areas per chamber to accommodate the twenty-four electron detectors in the whole ring. Conflat access ports are provided at the inner radius of the chambers for pump connections and installation of various internal components. A short rectangular aluminum bellows adaptor is placed between the chambers. This bellows allows for the installation of the chambers and for the alignment of the end flange clamps and seals which are only accessible from the inside of the ring. The end flange clamps consist of two vertical V-shaped clamps jointed together with 4 horizontal titanium rods on the top and bottom planes. Viton O-rings are used due to the limited sealing force produced by the clamps through the tightening of the titanium rods.

## **DISCLAIMER**

**Portions of this document may be illegible  
in electronic image products. Images are  
produced from the best available original  
document.**

The sector chamber is a welded fabrication of 6061 aluminum alloy plates. The top and bottom plates are 13.5 mm thick and the side walls are 19 mm thick. The wall adjacent to the detectors is only 3 mm thick thus minimizing the energy loss of the electrons. After machining and chemical cleaning, the plates are joined together with outside welds on a 4 m long weld fixture table in a clean room. The post-weld flatness is approximately 1 mm. The top and bottom surfaces are then machined to a flatness of 0.25 mm. The Conflat access port flanges and the rectangular end flanges are then welded on.

Four electrostatic quadrupoles, each occupying one and half sector chambers (equal to 39 degrees of the circumference) as shown in Fig. 2, are used to focus the injected muons. They are pulsed at  $\pm 27$  kV during the storage period. The electrodes are mounted on the curved support frames which are installed inside the sector chambers through the end flanges. The support frames cover the entire ring and are made from extruded aluminum. The electrodes are fabricated from aluminum, titanium, alumina and macor. The cross sectional view of the chamber, the support frame and the electrodes are shown in Fig. 4. A nuclear magnetic resonance (NMR) trolley containing up to 25 NMR probes sealed in an aluminum cylinder will be used periodically to map the magnetic field of the storage region around the ring. This NMR trolley operates within storage ring vacuum and is pulled by two coaxial cables. The trolley will ride on the corner rails of the support frame, and will be parked in a 'garage' when not in use. The coaxial cables will be guided by polypropylene wheels mounted on the support frame. The cables will transmit power and signals for the NMR probes. There are also 30 fixed NMR probes mounted in external grooves in the upper and lower plates of each sector chamber.

### III. VACUUM EVALUATION OF THE SECTOR CHAMBERS

After fabrication and cleaning, the chambers are pumped down, leak checked and

measured for deflection of the top/bottom plates under vacuum load. The deflection of the top plates of the prototype chamber at its widest span was found to be 0.45 mm. This is in agreement with the calculated value of 0.4 mm using ANSYS finite element code.<sup>3</sup>

Without a large on-site chemical cleaning facility, the completed sector chambers were cleaned with pressurized hot water spray mixed with mild-etch alkaline detergent, rinsed with hot water followed by drying in an air oven. The effectiveness of the cleaning steps can be evaluated by measuring the outgassing of the chambers. The outgassing rates of the sector chambers after various cleaning treatments were measured using the 'standard orifice method'. They are plotted versus the pumpdown time in Fig. 5. After hot water rinse, no significant changes in total outgassing rates were observed, however drastic reduction in hydrocarbon contaminations were observed when monitored with a quadrupole residual gas analyzer. The outgassing after mild alkaline etch (pH = 11.5) was found to be lower than that with strong alkaline etch (pH = 12.5). This is consistent with previous report<sup>4</sup> of a thicker oxide layer formed after heavy etching. An outgassing rate of mid  $10^{-10}$  Torr.l/sec.cm<sup>2</sup> can be reached one day after pumpdown with mild-etch detergent rinse. The slopes of the outgassing curves are consistent with  $Q = Q_0 t^n$  with  $n \sim 1.1$  which is the characteristics of the outgassing of water.<sup>5</sup>

#### IV. DISTRIBUTED ION PUMPS AND PRESSURE DISTRIBUTION

The injected muons are stored for a few milliseconds while they decay into electrons, neutrinos and gamma rays. A medium vacuum of  $10^{-3}$  Torr is sufficient when considering the beam loss due to muon-residual gas interaction. However, to minimize electron trapping at the quadrupole electrodes by the magnetic field and high voltage breakdown, a pressure of  $10^{-7}$  Torr is needed especially when  $\mu^-$  particles are stored. During the  $\mu^-$  mode of operation, the top and bottom electrodes will be at -27 KV and side electrodes at +27 KV.

Sputter ion pumps are usually employed in accelerator vacuum systems. However conventional lumped ion pumps cannot be used near the vacuum chambers due to the magnetic field uniformity requirement. Distributed ion pumps(DIP), utilizing the bending field of the superconducting magnet to confine the Penning discharge, have been selected as the main high vacuum pumps. Two locations of 5 cm by 50 cm in each chamber (as shown in Figures 3 and 4) are out of the path of the decay electrons and are available for the installation of DIPs. The magnetic field at these locations ranges from 12 to 15 KG. The pumping speeds of several ion pump elements of various geometries at high magnetic fields have been studied.<sup>6</sup> Elements with anode radii of 5 - 6 mm were found to have the highest pumping speed at fields above 10 KG and were selected for g-2.

The design of the g-2 DIPs is shown in Fig. 6. Two units of DIPs can be fitted at each 5cm x 50cm area. Each unit consists of three layers of cells of approximately 25 cm long, 5 cm wide and 10 cm high. The DIPs can be installed or retrieved through the downstream conflat flange port. Both the anodes and the cathodes are fabricated from titanium. The anodes have a cell radius of 5.5 mm and cell length of 19 mm. The pumping speeds per cell of the prototype DIP at various magnetic fields and pressures are shown in Fig. 7. With a total of 140 cells, each DIP unit will have pumping speed of over 50 l/sec and a total pumping speed of over 2000 l/sec for the whole ring. The discharge current of the DIPs will be used to measure the vacuum levels around the ring since no commercial ionization gauges are suitable for this application.<sup>7</sup> The commercially available high voltage feedthroughs use nickel plating and Kovar as transitions between ceramic and stainless steel. Kovar has a very high magnetic susceptibility and is not acceptable here. Instead, the feedthroughs will have aluminum as center conductor, transition and flange material. The aluminum is brazed to alumina insulator using Mo-Mn metallizing, aluminum plating and aluminum alloy brazing.

The DIPs will not be installed during the commissioning stage in early 1996. The storage ring vacuum will be pumped down and maintained with two 360 l/sec turbomolecular pumps located at opposite sides of the ring. The turbomolecular pumps will be positioned three meters radially away from the storage region, which reduces the effective pumping speed to less than 200 l/sec. The long aluminum manifolds are necessary to minimize the disturbance of the field uniformity at the storage region by the pump stations.

The pressure distribution at the storage region is simulated using a Monte-Carlo program<sup>8</sup> 'Molflow'. The results are plotted in Fig 8 versus the azimuthal length of the sector chamber. Without DIPs, a pressure of low  $10^{-6}$  Torr will be reached one day after pumpdown and low  $10^{-7}$  Torr with DIPs. Excessive breakdown of the high voltage has been observed at  $10^{-6}$  Torr during the testing of the prototype quadrupole electrodes operating at  $\mu^-$  mode (with top and bottom electrodes at negative voltage). This limits the experiment to  $\mu^+$  modes during commissioning. The  $\mu^-$  modes are only possible with the installation of the DIPs.

## V. SUMMARY

Due to the unique physics requirement of the g-2 experiment, all the vacuum components must be fabricated from materials with very low magnetic susceptibility. The vacuum chambers are fabricated from 6061 aluminum plates. The dimensional tolerances of the completed chamber are within the design values. The measured deflection of the prototype chamber under vacuum load is in agreeable with the ANSYS analysis. The outgassing rate of the chamber after cleaning with mild etching detergent is adequate. Prototype distributed ion pump elements with titanium anodes and cathodes have been tested and found to provide sufficient pumping speed at high magnetic field. With distributed ion pumps, the pressure distribution around the quadrupole electrodes will be sufficiently low one day after pumpdown for their reliable operation.

## Figure Captions

Fig. 1. The cross sectional view of the 45 m continuous superconducting magnet, its three cryostats and the muon storage chamber.

Fig. 2. The layout of the muon storage ring vacuum system without the superconducting magnet, consisting twelve sector chambers (ten standard and two special for inflector magnet and for NMR trolley garage), Q1 to Q4 represent the four quadrupole electrode sections.

Fig. 3. The design of the standard sector chamber together with distributed ion pumps and turbopump manifold. The stepped areas are for electron detectors.

Fig. 4. The cross sectional view of the sector chamber at its widest point. The rectangular frame supports the quadrupole electrodes and provides the rails for NMR trolley. Dimensions are in cm.

Fig. 5. Outgassing rates of the prototype sector chamber after various cleaning treatments. The designed outgassing rate of  $1 \times 10^{-9}$  Torr.l/sec.cm<sup>2</sup> at t = 24 hrs. can be reached after cleaning with mild-etch detergent.

Fig. 6. The design of the g-2 distributed ion pump elements consisting of a three layered structure with titanium anodes and cathodes. The anode cell radius is 5.5mm and cell length 19 mm. Each element have 144 cells.

Fig. 7. The pumping speed of the g-2 prototype distributed ion pump as a function of magnetic field and pressure.

Fig. 8. Monte-Carlo simulation of the pressure distribution inside the quadrupole electrodes using 'Molflow' with 2 turbopumps; and with 24 distributed ion pumps. The x-axis represents the azimuthal length of the chamber. Total number of molecules generated in the simulation is approximately 30,000 per sector chamber.

## References

<sup>1</sup>V.W. Hughes, *Particle, Strings & Cosmology* (World Scientist, Singapore, 1992), p. 868.

<sup>2</sup>W.M. Morse, g-2 Tech. Note No. 175, Nov. 1993(unpublished).

<sup>3</sup>ANSYS code, ver. 5.0, Swanson Analytical Systems Inc., Houston, PA.

<sup>4</sup>R.A. Rosenberg, M.W. McDowell and J.R. Noonan, *J. Vac. Sci. Technol.*, **A12**, 1755(1994).

<sup>5</sup>H.F. Dylla, D.M. Manos and P.H. LaMarche, *J. Vac. Sci. Technol.*, **A11**, 2623(1993).

<sup>6</sup>H.C. Hseuh, W.S. Jiang and M. Mapes, *J. Vac. Sci. Technol.*, **A13**, 531(1995).

<sup>7</sup>H.C. Hseuh, W.S. Jiang and M. Mapes, *J. Vac. Sci. Technol.*, **A12**, 1722(1994).

<sup>8</sup>A PC based Monte Carlo simulation program for vacuum systems written by Roberto Kersevan, Sincrotrone Trieste, ST/M-91/17, September, 1991(unpublished).

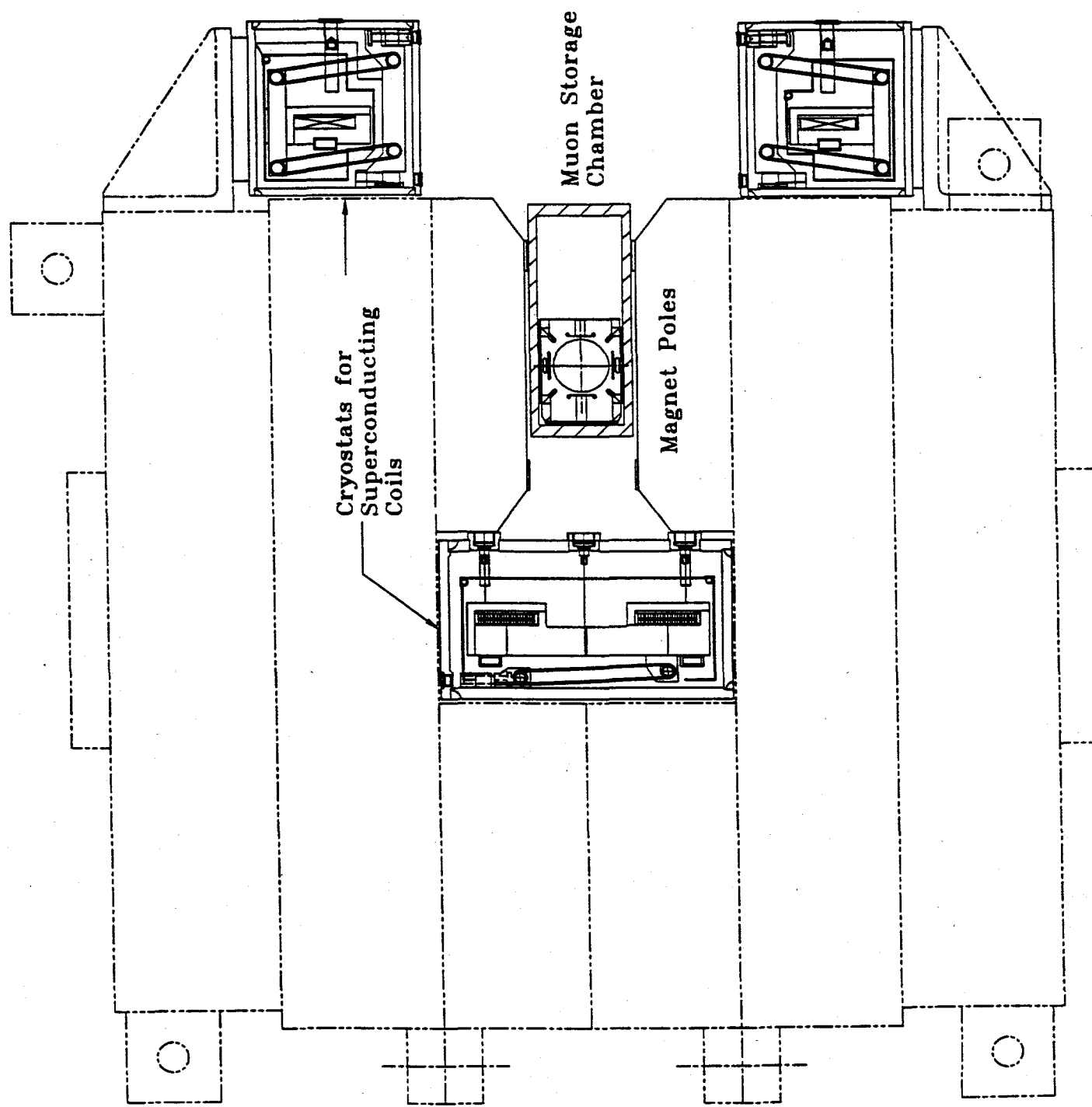


Figure 1.

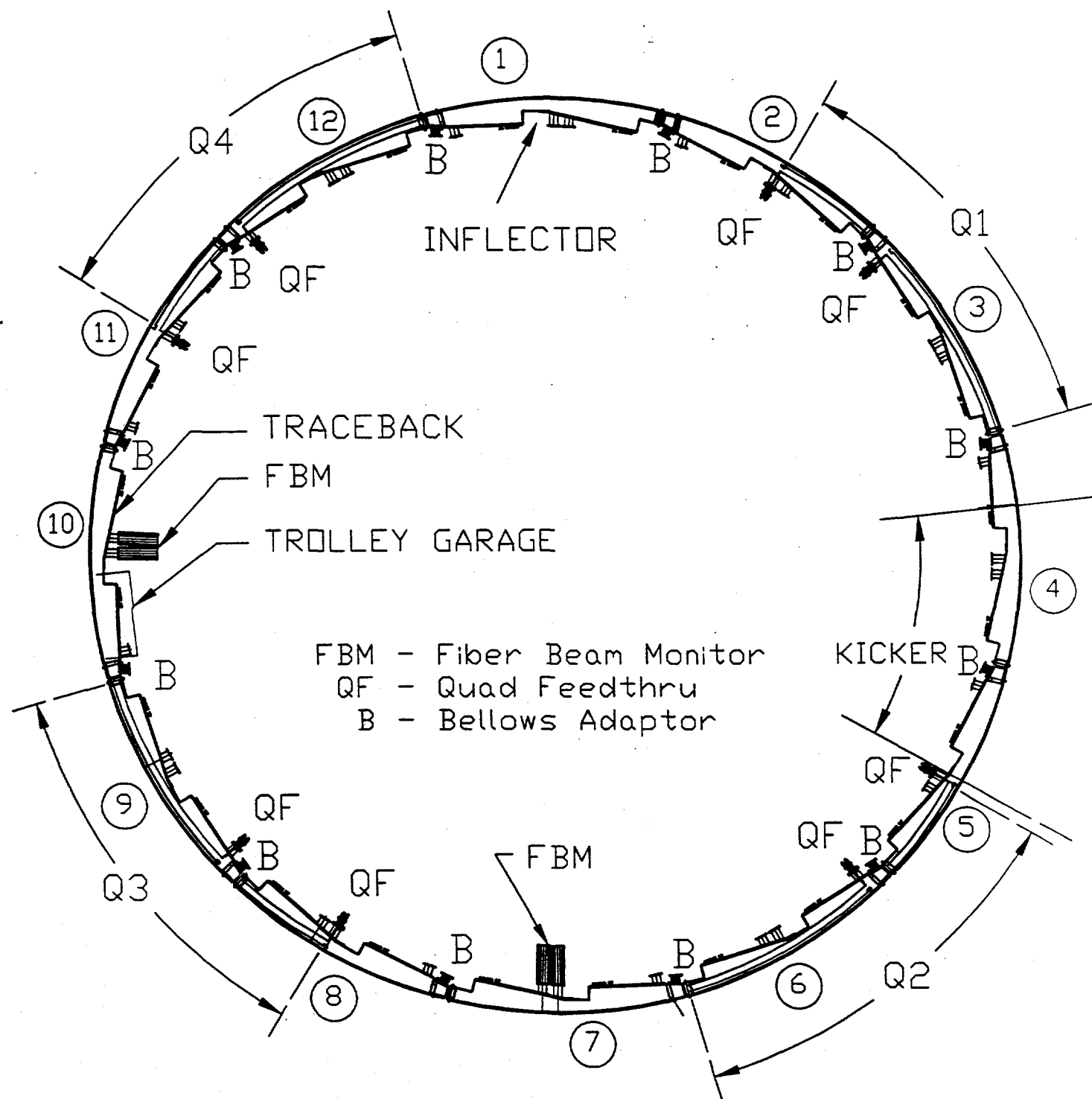


Figure 2.

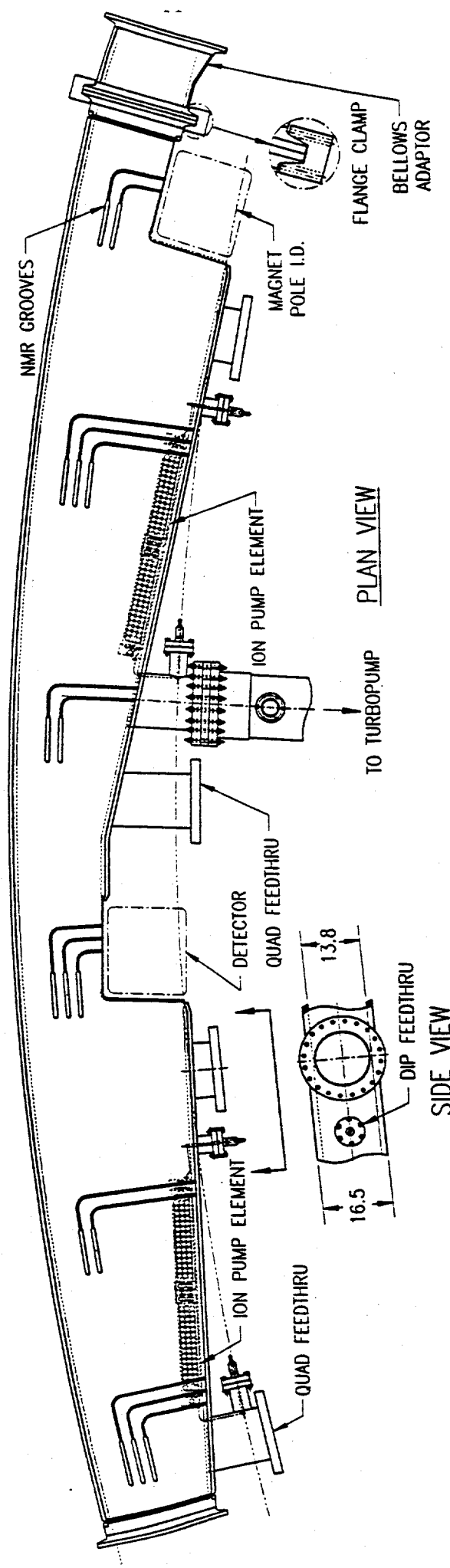


Figure 3.

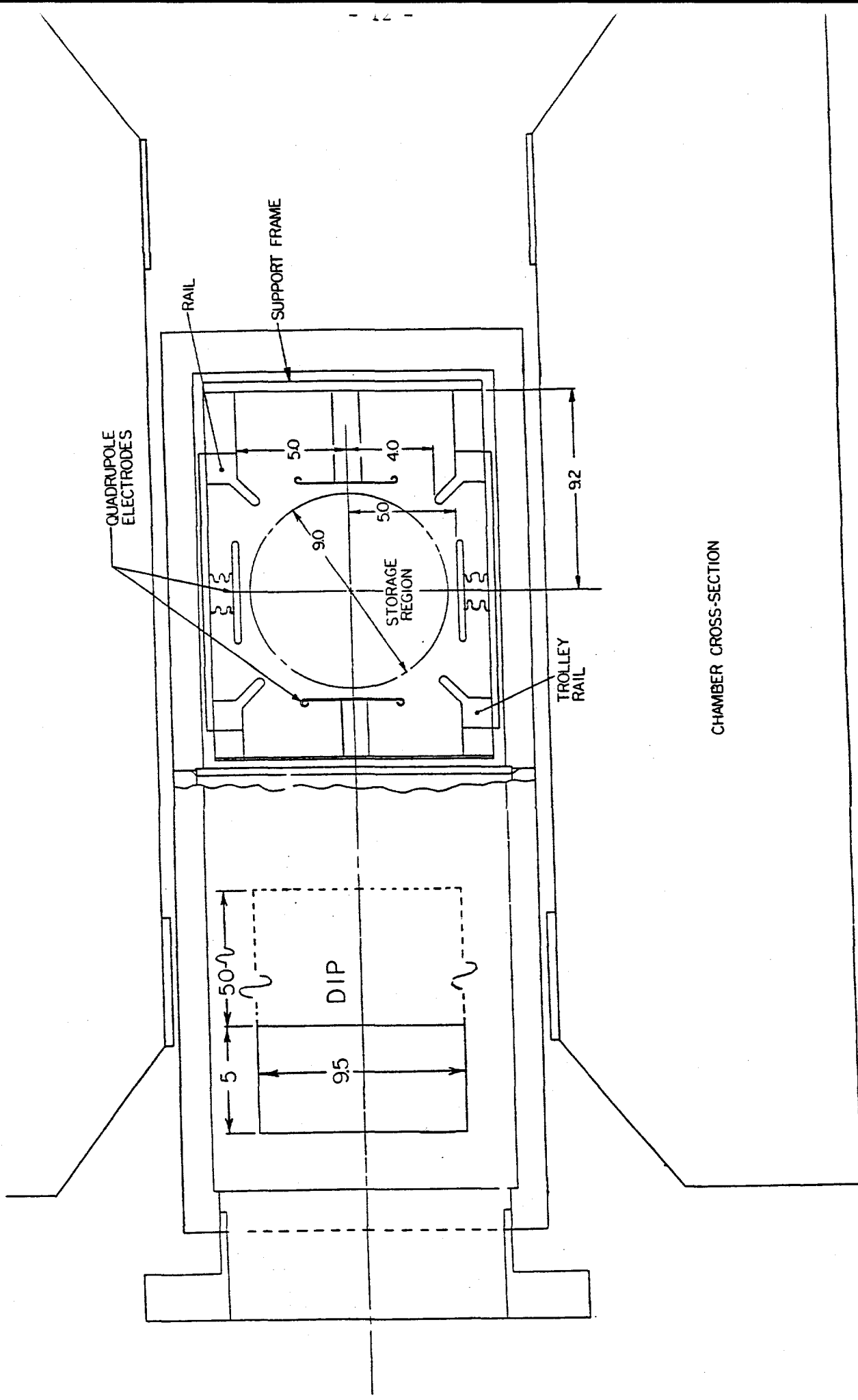


Figure 4.

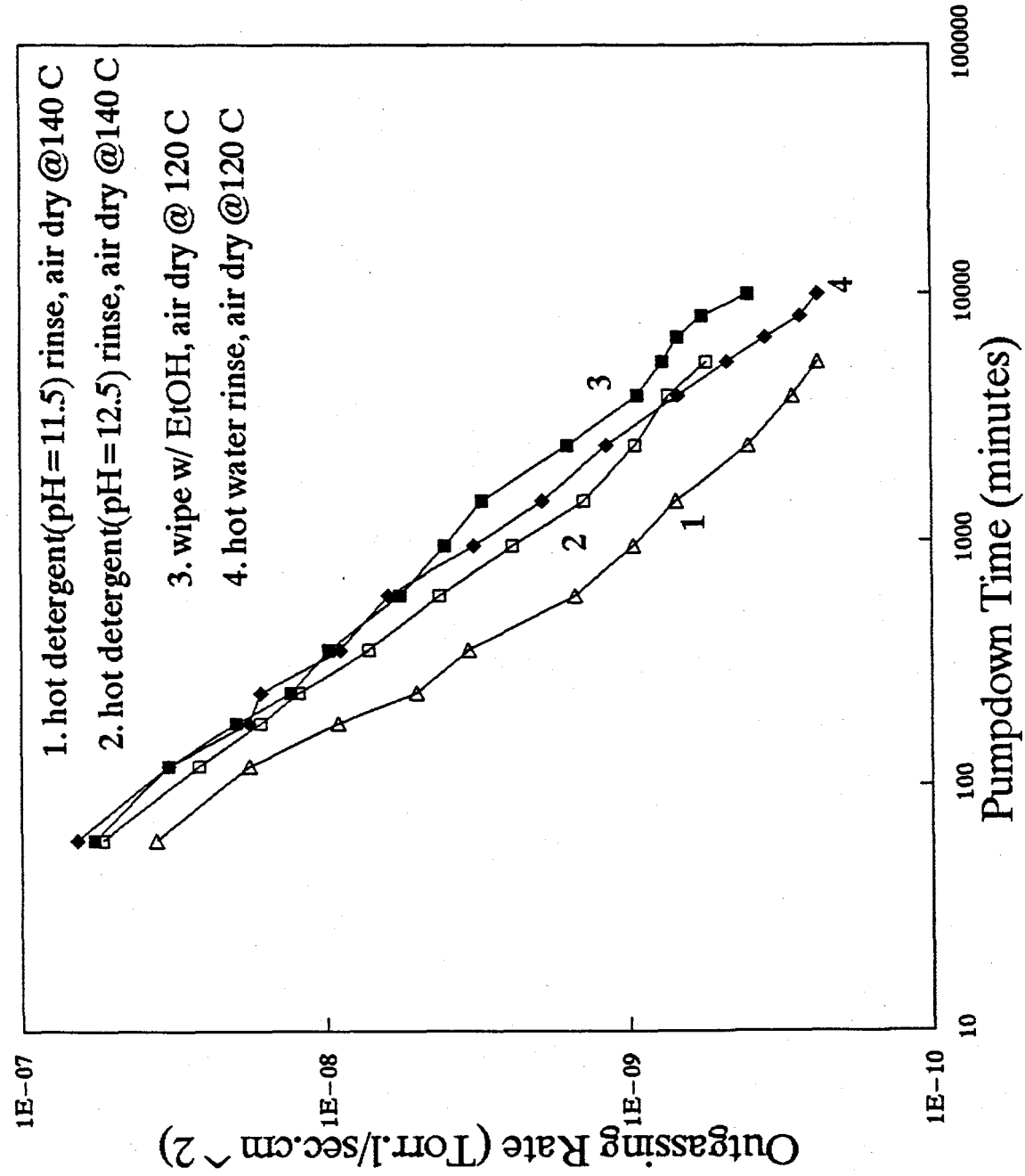


Figure 5.

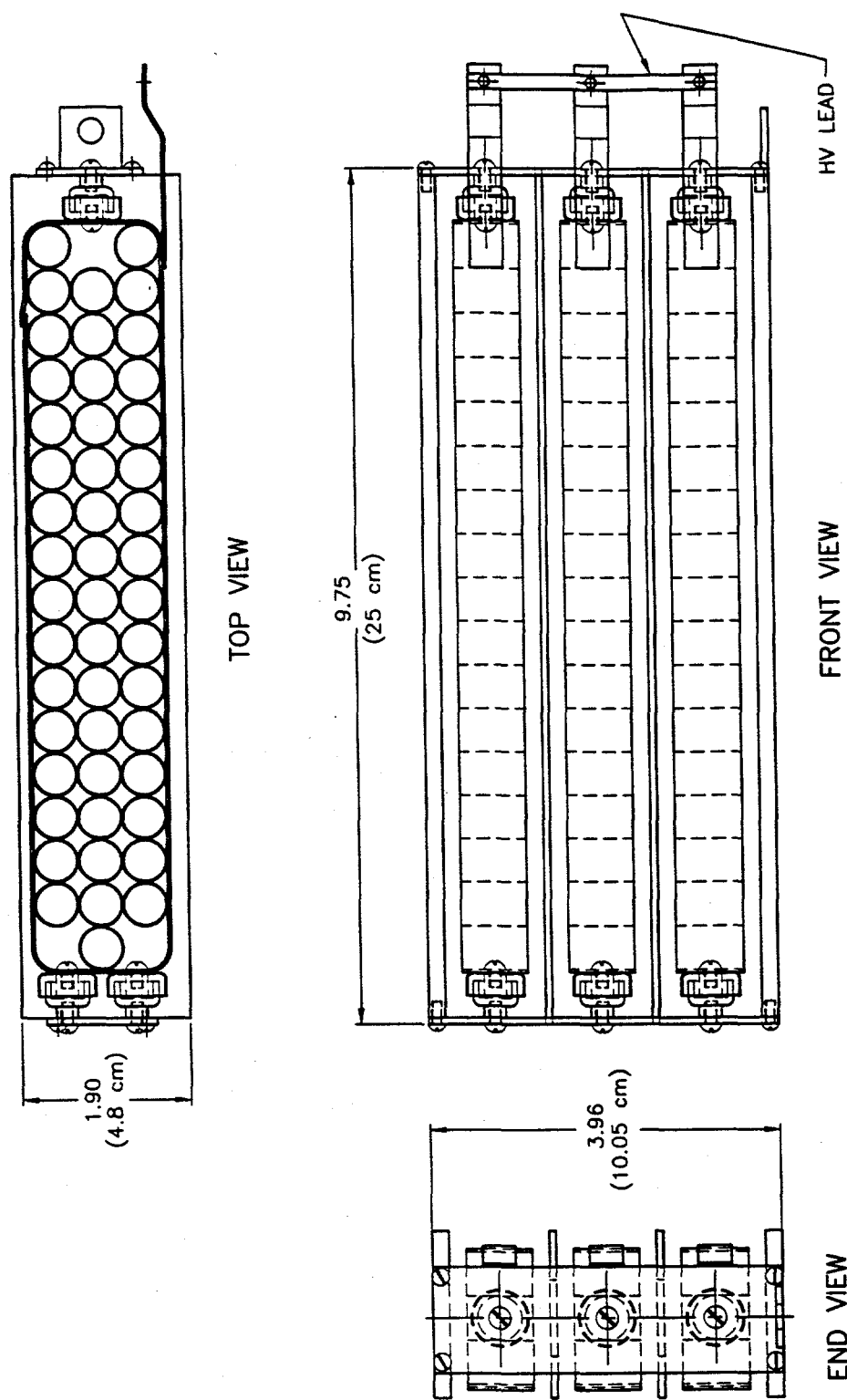


Figure 6.

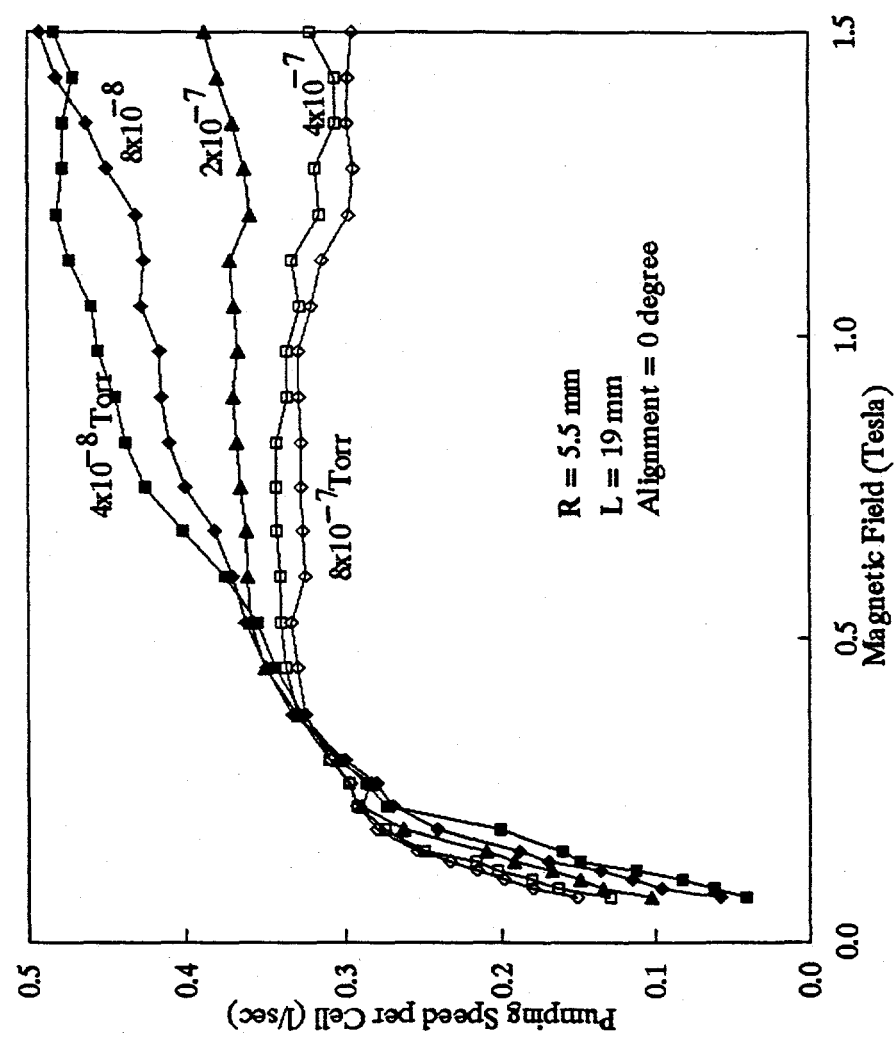


Figure 7.

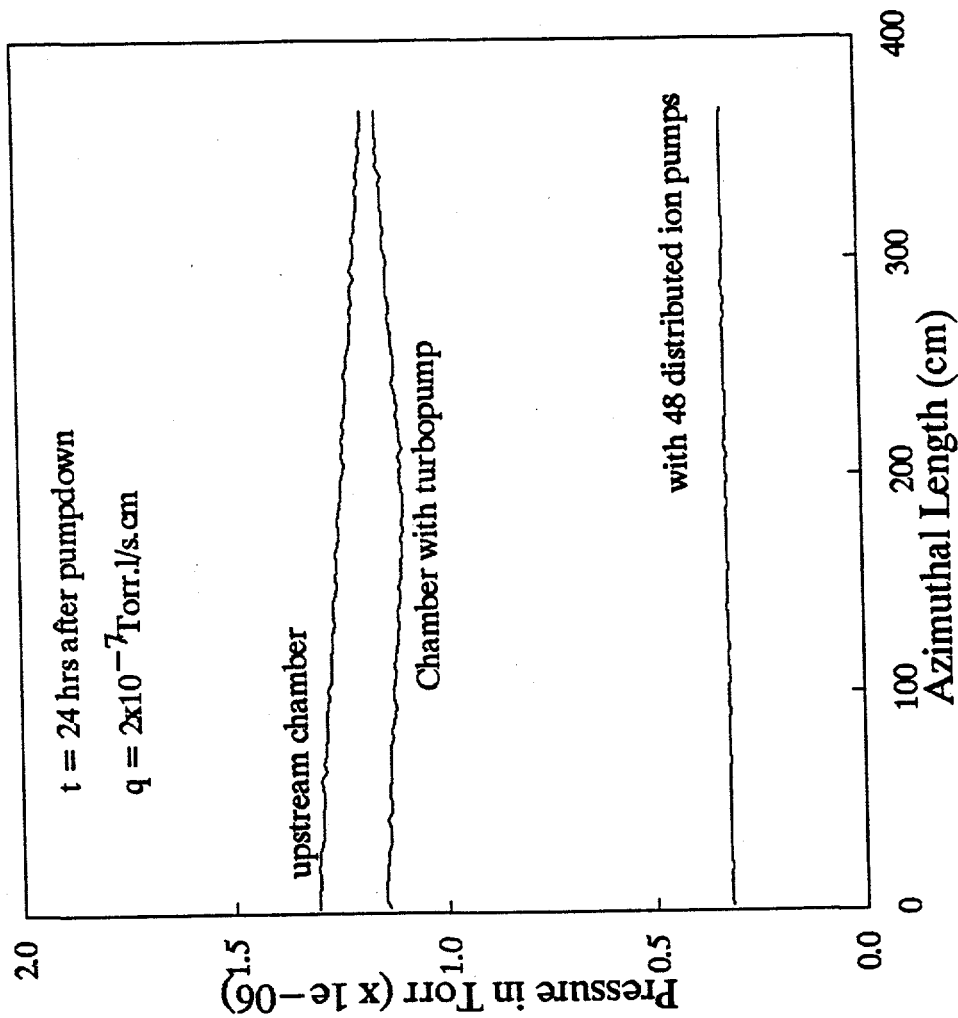


Figure 8.

#### DISCLAIMER

This report was prepared as an account of work sponsored by an agency of the United States Government. Neither the United States Government nor any agency thereof, nor any of their employees, makes any warranty, express or implied, or assumes any legal liability or responsibility for the accuracy, completeness, or usefulness of any information, apparatus, product, or process disclosed, or represents that its use would not infringe privately owned rights. Reference herein to any specific commercial product, process, or service by trade name, trademark, manufacturer, or otherwise does not necessarily constitute or imply its endorsement, recommendation, or favoring by the United States Government or any agency thereof. The views and opinions of authors expressed herein do not necessarily state or reflect those of the United States Government or any agency thereof.